Molecular BioSystems

Dynamic Article Links

Cite this: *Mol. BioSyst.*, 2011, **7**, 2599–2607

www.rsc.org/molecularbiosystems

PAPER

Small delay, big waves: a minimal delayed negative feedback model captures *Escherichia coli* single cell SOS kinetics†

Lennart Hilbert,*[ab] David Albrecht[c] and Michael C. Mackey[d]

Received 29th March 2011, Accepted 3rd June 2011
DOI: 10.1039/c1mb05122a

Background: How exactly does an organism coordinate its responses to differing environmental conditions, especially when several responses and physiological priorities are potentially conflicting? Recently, single cell results have been published on the kinetics of the bacterial SOS response. Based on these, we construct a relatively simple mathematical model for the regulatory control of the mutagenic elements of the *Escherichia coli* DNA repair system. *Methods:* We employ one first order delay differential equation for the dynamics of the activation level of mutagenic gene repair and one first order ordinary differential equation for the dynamics of the level of DNA damage. After manual adjustment of parameters, our model qualitatively reproduces the UV dose dependent RecA expression peak occurrence, peak amplitude and peak timing. Parameter noise captures qualitatively the fluctuations observed in the experimental data. Quantitative agreement is achieved for timing of the three response peaks for different doses of UV. *Conclusions:* A delayed negative feedback is likely to play a primary role in the regulation of the *E. coli* mutagenic gene repair. The model presented in this paper is an example of how a delayed regulatory mechanism establishes control over a critical organismic response with negative secondary effects.

1 Introduction

For any organism, the integrity of its hereditary information, the genome, is crucial. Damage can manifest itself through changes of the contained information, *i.e.* genetic mutations, or as physical damage to the information carrier itself. Both types of damage readily occur and are therefore a possible evolutionary origin of the molecular mechanisms that safeguard genetic information as well as the physical information carrier. Understandably, both aspects of gene repair are of high physiological priority, but situations where they are in conflict can and do occur.

Published experimental data[1] give insight into how the interplay of these gene repair priorities shapes the regulatory dynamics of the *E. coli* SOS response (a bacterial DNA repair system which can counteract consequences of physical DNA damage very effectively at the cost of allowing more mutations than conventional repair). Based on these data from specific model organisms, mathematical modeling can give detailed insight into the more general question of how physiological priorities are condensed into actual regulatory mechanisms. Mechanistic models[2,3] can give detailed account of regulation in a specific model organism or experimental setup. In contrast, the abstraction of general concepts from a specific experimental context favors conceptual, minimal models. Such a minimal model of the experimentally observed *E. coli* SOS response[1] is still missing.

In this paper, we develop a simple delayed negative feedback model for the single cell expression kinetics of the *E. coli* SOS response after UV irradiation.[1] This minimal delay model captures the observed SOS expression kinetics more comprehensively than existing mechanistic models.[2,3] Further, it is an example of the precise adjustment of a critical organismic response with negative secondary effects to a specific stress level. The regulation is established through delayed feedback and delayed induction.

SOS response

When physical damage to an organism's information carrier occurs, repairing it quickly is the highest priority. The repair is executed even if it compromises another priority, the integrity

[a] *Department of Physiology, Centre for Applied Mathematics in Biosciences and Medicine, McGill University, McIntyre Medical Building, 3655 Promenade Sir William Osler, Montreal, Quebec, Canada. E-mail: lennart.hilbert@mail.mcgill.ca; Fax: +1 514 398-7452; Tel: +1 514 398-8224*
[b] *Meakins-Christie Laboratories, McGill University, 3626 Rue St. Urbain, Montreal, Quebec, Canada*
[c] *Institute of Biochemistry, ETH Zurich, Schafmattstrasse 18, Zurich, Switzerland*
[d] *Departments of Physiology, Physics and Mathematics and Centre for Applied Mathematics in Bioscience and Medicine, McGill University, 3655 Promenade Sir William Osler, Montreal, Quebec, Canada*

† Electronic supplementary information (ESI) available: MatLab scripts to produce displayed simulation results. See DOI: 10.1039/c1mb05122a

of the genetic information. The SOS response was first described more than 35 years ago.[4] Its mechanisms to either bypass or repair DNA damage have since been investigated extensively in *E. coli* as a model organism. Including more than 40 genes, the SOS response counteracts DNA damage in various ways, including nucleotide excision repair (NER), homologous recombination, translesion DNA replication and cell cycle arrest.[5]

The SOS response elements range from non-mutagenic to highly mutagenic. Accordingly, the regulation of the SOS response can be seen as a bacterium's means to finely balance between informational and physical integrity of the genome. Expression of the proteins involved is regulated by the repressor LexA. LexA binds with differential affinity to the promoter regions of the different SOS genes, termed SOS boxes. Under normal growth conditions, each gene is expressed at a basal level, which is set by a gene's SOS box's specific complementarity and resulting binding affinity for the LexA protein.[6] DNA damage sensing is mediated by an effective yet simple mechanism. During replication, replication forks stall upon encountering lesions in the DNA. The exposed single stranded DNA is recognized by RecA, which binds to it and is changed into the active form RecA*. This in turn catalyses self cleavage of LexA, inducing the expression of the previously repressed SOS genes. For further background information reviews should be consulted.[7,8]

The temporal induction of the different SOS response genes occurs in a stepwise fashion. First, proteins involved in NER are expressed and begin to remove damaged nucleotides. Subsequently, homologous recombination is increased and finally, the DNA polymerase PolV, which is error-prone yet capable of translesion repair, becomes active.[9] In this way the SOS response is initiated by minimal DNA damage, but the mutagenic repair action of PolV only takes effect if damage still persists after the time delay between initiation and PolV repair action. As a consequence, the induction of the SOS response only leads to disruption of genetic information if DNA lesions cannot be repaired in the delay time corresponding to PolV activation. This regulation pattern allows for the mutagenic SOS response to be sharply controlled, and thus to reduce the genetic mutations to a minimum.[5] Of more general interest, the SOS response has drawn attention because it displays bursts of genetic variability at the cost of replication fidelity,[10] a concept that is widely conserved in *E. coli*.[11]

Experimentally observed SOS kinetics

Friedman *et al.*[1] irradiated *E. coli* with doses of 10 to 50 J m^{-2} of UV light and monitored the resulting activation of the SOS response in single cells. As a reporter system, low copy plasmids were introduced, which contained a promoterless GFP gene after the LexA repressed promoter regions of *recA*, *lexA* and *umuDC*, the latter encoding the UmuD and UmuC subunits of polymerase PolV. When monitored at the single cell level, the normalized promoter activity appeared in discrete peaks after irradiation. The timing of the peaks was conserved throughout the cells in one population. For increasing doses of UV light, peak amplitudes saturated and the number of observed peaks and the delay between individual peaks increased.

2 Model development and adjustment to data

General approach

Our model is based on data and findings of Friedman *et al.*[1] We take into consideration a limited set of aspects of the regulation of PolV expression and repair activity: (1) delayed initial induction only by a persistent signal indicating physical DNA damage, (2) a sharp shut-down when physical damage has been cleared, and (3) a delay time τ from replication fork stalling to the actual repair activity of PolV. A visual representation of the model and example traces for the simulation of a single cell is shown in Fig. 1.

Mathematical formulation

We propose a minimal mathematical model that combines the aforementioned aspects of mutagenic SOS repair. We employ two dynamic variables. $E(t)$ represents the current activity of mutagenic SOS repair, where $E = 0$ corresponds not to no activity, but to a base level of signaling without external UV irradiation. $D(t)$ monitors the actual amount of physical genome damage present in the cell; note that the amount of damage sensed by stalled replication forks generally differs from but depends on $D(t)$.

Clearance of physical DNA damage *D*. For the sake of simplicity we assume that non-mutagenic repair contributes only negligibly to the reduction of physical DNA damage, the reduction is instead governed by the levels of physical damage $D(t)$ itself and by $E(t)$, the current activity of mutagenic repair. We describe the repair of physical DNA damage by

$$\frac{\mathrm{d}D}{\mathrm{d}t} = -C_r \max\left\{\frac{D(t)}{1+D(t)}, 0\right\} \times \max\left\{\frac{E(t)}{1+E(t)}, 0\right\}, \quad (1)$$

where C_r is a constant coefficient describing the rate at which mutagenic SOS repair removes physical DNA damage. The Hill-type functions including $D(t)$ and $E(t)$ account for our assumption that mutagenic repair of physical DNA damage is increased by the presence of more physical damage as well as by stronger induction of the mutagenic repair, while it has a limited capacity that leads to saturation with increasing $D(t)$ and $E(t)$. The $\max\{\ldots,0\}$ expressions serve to prevent non-physiological undershoots, which would correspond to the mutagenic SOS repair adding surplus physical damage.

Note that both Hill-type functions take on the half-value at $K_D = 1$ and $K_E = 1$. We can, and indeed should, simplify our model formulation in this way, as K_D as well as K_E can be scaled into D and E and the model parameters (namely C_r, γ_0, and s_0) without loss of generality; they are redundant parameters, which if kept lead to over-parametrization of the model. For example purpose, let us rescale, starting with non-scaled $\bar{D}(t)$ and $\bar{E}(t)$ with respective half-values k_d,k_e:

$$\frac{\mathrm{d}\bar{D}}{\mathrm{d}t} = -\bar{C}_r \frac{\bar{D}}{k_D + \bar{D}} \frac{\bar{E}}{k_E + \bar{E}}; D := \bar{D}/k_D,\ E := \bar{E}/k_E$$

$$\Rightarrow \frac{\mathrm{d}D}{\mathrm{d}t} = -C_r \frac{D}{1+D} \frac{E}{1+E},\ C_r = \bar{C}_r/k_D.$$

The rescaled half values are now 1.

This journal is © The Royal Society of Chemistry 2011

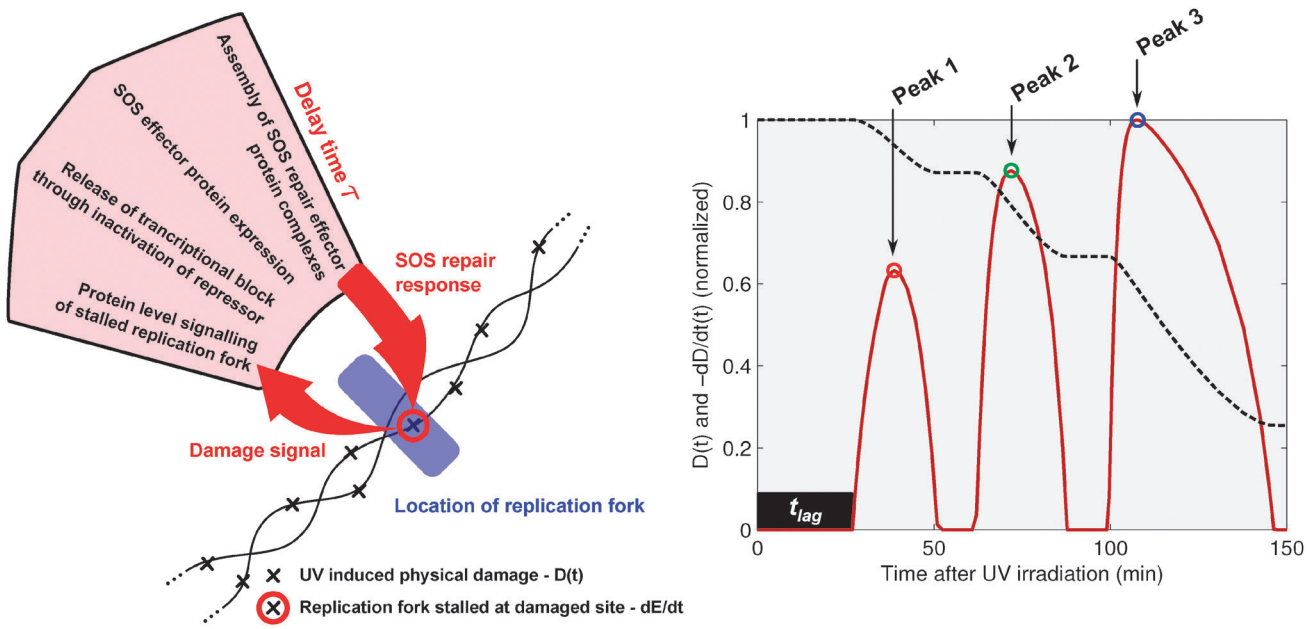

Fig. 1 Model overview and single cell example simulation results. The left diagram depicts the basic elements of the model. The two interwoven black lines represent a piece of a longer DNA strand, which is undergoing replication. Black **x** symbols are UV-induced physically damaged sites on the DNA strand. The blue-shaded rectangle on the DNA strand is the current position of a replication fork. The replication fork is stalled by a damaged site, the stalling is indicated by a red circle around the damaged site. From a stall point, signaling to the SOS response is indicated by a red arrow away from the stall point. The framed box contains a sequence of molecular events that likely is responsible for the time delay τ observed in experiment[1] and incorporated into our model. Finally, another red arrow indicates the SOS repair action, which frees the stalled replication fork. The right graph displays an example simulation trace of a single cell response to 50 J m^{-2} irradiation, model parameters as in Table 2. $D(t)$ (black dashed line) is the overall amount of physical DNA damage present. $\mathrm{d}D/\mathrm{d}t$ (solid dark red line) is the rate of clearance of this damage $D(t)$. The peaks of $-\mathrm{d}D/\mathrm{d}t$ were used to detect peaks in *recA* promoter activation. Peak 1, Peak 2 and Peak 3 are indicated by a red, a green and a blue circle, respectively. t_{lag} is the induction delay from an initial DNA physical damage signal to the first induction of the mutagenic SOS response.

RecA signaling. The rate of damage clearance $\mathrm{d}D/\mathrm{d}t$ is pivotal in the regulatory system; at any given time replication forks stall at sites of physical damage and are freed (mostly) by mutagenic SOS repair action (PolV). This dynamically sets the duration of replication forks being stalled at a site of physical damage. The longer a replication fork is stalled at one and the same site of physical damage, the stronger the signaling to the mutagenic SOS boxes (binding of RecA to single stranded DNA exposed by the stalled replication forks, activation of bound RecA into RecA*, cleavage of LexA, derepression of mutagenic SOS boxes). The rate of clearance thus sets the signaling strength to the mutagenic SOS repair, so we use $-\mathrm{d}D/\mathrm{d}t$ as an indicator of *recA* promoter activity, the first experimentally detectable element in the signaling chain.[1]

Current mutagenic repair activity *E* is dynamically set by the damage level *D* and delayed mutagenic repair action E_τ. To complete our model, we have to describe the dynamic behavior of the current mutagenic SOS repair activity level $E(t)$, which is governed by both the damage level $D(t)$ and the action of mutagenic SOS repair by PolV.

First, let us only consider the influence of the damage $D(t)$ without mutagenic SOS repair. We assume that non-mutagenic repair is working at full capacity, which is insufficient to effectively prevent replication forks from stalling for long. We translate this assumption as a constant increase in the mutagenic SOS repair activity at a rate γ_0. However, mutagenic SOS repair activity is only observed after an initial period t_{lag} of non-mutagenic repair. Therefore we employ a Heaviside function $H(t - t_{\mathrm{lag}})$ to "switch on" mutagenic repair only after t_{lag}. We combine this into an expression describing the mutagenic SOS repair activity increase at saturated levels of damage $D \to \infty$ and not yet considering any effects of PolV repair action:

$$\gamma(t) = \gamma_0 H(t - t_{\mathrm{lag}}). \qquad (2)$$

For non-saturated damage levels $D < \infty$ we introduce a Hill-type pre-factor, so that a lower damage level leads to less repair action simply for the reason that less damaged sites are encountered by replication forks. Combining all these aspects, we can now write down a differential equation for $E(t)$, that does not yet incorporate the influence of mutagenic PolV repair action:

$$\frac{\mathrm{d}E}{\mathrm{d}t} = \max\left\{\frac{D^{n_d}}{1 + D^{n_d}}, 0\right\}\gamma(t). \qquad (3)$$

The influence of the damage saturates for $D \to \infty$. For more damaged sites present, replication forks stall more often. For increasing damage, however, an increasing fraction of all replication forks is stalled for an increasing fraction of time, so saturation is reached. In contrast to (1), a Hill-exponent n_d was introduced as this physical dependence might differ from the regulatory dependence on D described in (1).

PolV action reduces the stalling of replication forks by enabling translesion DNA replication, which in turn allows

the replication fork to pass the stall point. In our model this should lead to a reduction of the increase of E. As a multi-step molecular pathway containing at least two sequential regulations of transcription (*recA*, then *umuDC*), we assume a delay τ from signaling to mutagenic SOS repair till it actually takes effect by reducing the stalling of replication forks at sites of physical DNA damage. We place an additional term $-s_0E_\tau/(1 + E_\tau)$ into (3) to include mutagenic SOS repair with the above features. The term is placed along with $\gamma(t)$, which was employed earlier in (3), where mutagenic repair effects were not considered yet. We get

$$\frac{\mathrm{d}E}{\mathrm{d}t} = \max\left\{\frac{D^{n_d}}{1+D^{n_d}}\right\}\left[\gamma(t) - s_0\frac{E_\tau}{1+E_\tau}\right], \qquad (4)$$

where s_0 is a constant coefficient describing the relative strength of mutagenic SOS repair and $E_\tau = E(t - \tau)$ is the mutagenic SOS repair activity delayed by τ. Note that the half-value constant for the E_τ Hill-type function was set 1, by the earlier rescaling of E. The half-value in the D^{n_d} Hill-type function was assumed to be 1, solely for simplicity.

Initial conditions. $E(t \leq 0) = 0$ and $\dot{E}(t \leq 0) = 0$, because signaling to mutagenic gene repair is at a base level before irradiation. The initial damage level is set to $D(t = 0) = D_0$. In the experiment, the UV irradiation dose has been varied, and accordingly D_0 has to be varied in the initialization of our model according to the UV dose. We assumed a simple proportionality $D_0 = CI$, where C is a proportionality factor in units of [m^2 J^{-1}] and I the imposed UV dose in units of [J m^{-2}].

Model parameters

Delay time dependence on irradiation. From Friedman *et al.*[1] we can determine mean cell doubling times for different UV doses I, see Table 1. A quadratic fit using *Gnumeric* gives the following dependence:

$$T_D(I) = 0.0135\cdot I^2 + 0.599\cdot I + 39.0, \qquad (5)$$

with $R^2 = 0.9702$. The quadratic expression explained the experimental data better than a linear fit, for which $R^2 = 0.9481$. Further, Friedman *et al.*[1] show a strong correlation between cell doubling time T_D and the peak separation time T of the form

$$\frac{1}{T} = \left[\frac{1}{T_D} + \frac{1}{68\,\mathrm{min}}\right]. \qquad (6)$$

The oscillations observed in our model simulations have to match the time of peak separation T. Generally speaking, the oscillation period in oscillating delay system is strongly dependent on the feedback delay, called τ in our model.[12] Assuming a high damage limit $D_0 \to \infty$ and no induction delay $t_{\mathrm{lag}} = 0$, the core delay differential equation (4) becomes

$$\dot{E} = \gamma_0 - s_0\frac{E_\tau}{1+E_\tau}, \qquad (7)$$

which is of the type $\dot{E} = f(E_\tau)$, where only the delayed value of E is present in the right hand side. One steady state $E^* = \gamma_0/(s_0 - \gamma_0)$ exists when $s_0 > \gamma_0$. Linearizing around this steady state gives

$$\dot{u} = -S^*u(t - \tau),\ u(t) = E(t) - E^*, \qquad (8)$$

where $S^* = (s_0 - \gamma_0)^2/s_0$. This type of delay differential equation can be treated as shown elsewhere.[12] We assume that we are close to the Hopf bifurcation at which the first eigenvalue crosses to the positive real half of the complex plane. For combinations of (τ,s_0,γ_0) close to that bifurcation, either slowly decaying or persistent oscillatory behavior around E^* can be observed, with a period close to the Hopf period $T_{\mathrm{Hopf}} = 4\tau$. As our model should produce oscillations with a period of T to comply with the data, we investigated values close to $\tau = T/4$. We found $\tau = T/4.35$ to give good results. Using (5) and (6) we find

$$\tau = \frac{68\,\mathrm{min}}{4.3}\frac{T_D(I)}{68\,\mathrm{min} + T_D(I)}. \qquad (9)$$

Lag time dependence on delay time. For the lag time $t_{\mathrm{lag}} = 3\tau$ has been assumed, which makes the first peak time T_1 roughly T.

Further model parameters. The values of the other model parameters γ_0, s_0, C_r, n_d and C have been determined manually to mimic several features of the experimental data reasonably well, see Results and Discussion. Specifically, we considered the amplitudes and the occurrence of the discrete peaks during a heuristic search. First, γ_0 was picked, then a value $s_0 > \gamma_0$, then the three parameters C_r, n_d, and C were adjusted, see Table 2. While these parameters reproduce the aforementioned features, they are not necessarily optimal or even unique in any sense.

Biological fluctuations

For a comparison of model and data we include biological variations. We account for them by randomization of the model parameters for the regulation delay τ, the relative strength of mutagenic SOS repair s_0, and the initial damage value D_0. For each simulation of an individual cell we draw them from a normal distribution in the following manner:

$$\tau = \bar{\tau} \times (1 + N(0,\sigma_\tau)), \qquad (10)$$

$$s_0 = \bar{s}_0 \times (1 + N(0,\sigma_s)), \qquad (11)$$

$$D_0 = \bar{D}_0 \times (1 + N(0,\sigma_D)), \qquad (12)$$

Table 1 Mean cell doubling times T_D for different UV doses I as reported by Friedman *et al.*[1] The error of read-out from the graph shown by Friedman *et al.*[1] on cell doubling times is 5 min. Delay times τ as calculated from fitted cell doubling times $T_D(I)$ for different UV doses, see (5), and using eqn (9) describing the dependence of τ on the cell doubling time

I/J m^{-2}	0	10	20	35	50
T_D/min	37.5	46.5	62	70	105
τ/min	5.76	6.41	7.17	8.37	9.51

Table 2 Model parameter values: the parameter values have been determined manually, so as to capture reasonably well the experimental data from Friedman *et al.*[1]

Parameter	γ_0	s_0	C_r	n_d	C
Unit	1 min^{-1}	1 min^{-1}	1 min^{-1}	1	m^2 J^{-1}
Value	0.1	0.37	0.1	3	0.11

This journal is © The Royal Society of Chemistry 2011

where $N(\mu = 0,\sigma)$ is a normally distributed random variable with mean μ and variance σ, while $\sigma_\tau,\sigma_s,\sigma_D$ are the variances for the respective parameters. $\sigma_\tau = 0.03$, $\sigma_s = 0.2$ and $\sigma_D = 0.05$ are used where noise on the simulation parameters is employed, unless other values are mentioned.

At the risk of stating the obvious: the simulation itself is fully deterministic, only the parameters that initialize the simulation are picked randomly.

Numerical solutions

The differential equations were integrated with the *MatLab* integrator tool *ddesd*.[13] Our simulation code can be found in the ESI.†

3 Results

Wild type results

Peak distributions. In the original experiment[1] as well as in our model simulations wild type cells were exposed to UV doses of 20 and 50 J m^{-2}. In Fig. 2 peak distributions and histograms from the model and the experiment are shown for both conditions. A good quantitative agreement of the mean peak times is reached. With respect to peak amplitude and timing, the distributions agree qualitatively.

For a dose of 50 J m^{-2}, the first peak time and amplitude are confined to a small range. For the second and third peak fluctuations increase, especially those of the peak amplitude.

For a dose of 20 J m^{-2}, the fluctuations increase similar to those seen for the higher UV dose. The mean amplitudes, however, follow a different pattern. In the experimental data, the first peaks amplitude is exceeded by that of the second peak, while that of the third peak is lower than the two preceding ones. In our model results each consequent peak is decreased. A decreased number of cells exhibits a third peak, in the experimental data as well as in the histograms obtained from our simulations.

Peak occurrence, timing and amplitude. In Fig. 3 the different aspects of the SOS response peaks are displayed for experimental results from Friedman *et al.*[1] and simulations of our model. This more detailed and thorough comparison with data reveals strong qualitative agreement between model and experimental results. For higher UV doses, the number of cells exhibiting first, second and third peaks increases. The first peak is established throughout the monitored populations for irradiation of 10 J m^{-2} and higher. The second peak is more populated for doses higher than 10 J m^{-2} in experimental and model results. For 10 J m^{-2} irradiation the third peak is established in $\approx$15% of cells in the experimental data but not at all in the model results. Also, the third peak appears in almost all cells in the model after 50 J m^{-2}, while in the experimental results only 55% are reached. Still, the general pattern of consecutive increase of cells exhibiting one, two or all three peaks for increasing UV dose is visible in experimental as well as model results.

As observed in the experimental data, the mean peak times T_1, T_2 and T_3 are multiples of T throughout the whole irradation range above 10 J m^{-2}. The peak amplitudes saturate for an increase in UV dose; the first peak saturates first, followed by the second and then the third peak. In a Δ*umu* knockout system, the first peak amplitude increases with UV dose in experiment. The peak amplitude also reaches a higher value in the model results, but does not reach up as high as observed in the experiment, and exhibits a saturation behavior. As only two experimental Δ*umu* data points are available, conclusions on curvature and consequently saturation behavior cannot be drawn from the experimental data.

Effects of Δ*umuDC* on the feedback delay τ

For the Δ*umuDC* mutant bacteria, a more delayed and scattered second peak is observed, the third one is hardly present, see Fig. 4. To adjust our model, we increased the delay time τ by 90% (while not changing t_{lag}) and the associated variance σ_τ to 0.15. The increase in τ brings the timing of the second peak in alignment with the observations in the mutant experiment. This change in τ in our model is accompanied by an increase in the amplitude and time of the first peak. The same altered kinetics are found in the experimental observations, and have been shown to be a typical change resulting from increased delay times in a negative autoregulation in an engineered organism.[14,15] Thus, we suggest a prolonged delay time as an explanation of the expression kinetics observed in the Δ*umuDC* mutant experiment. The amplitude increase can also be viewed in Fig. 3. The increase in variance was introduced solely to reproduce the experimental results.

4 Discussion

Model evaluation and comparison with other models

Agreement with data and known mechanisms. Our model captures qualitatively most characteristics of the data presented by Friedman *et al.*[1] Most prominently, all three discrete *recA* promoter activity peaks are explained by a single delayed negative feedback loop. Correct coverage of a broad range of data is usually indicative for a model to have captured a good deal of the underlying dynamical system. In comparison, Krishna *et al.*[2] can explain a second response peak along with many detailed characteristics of the data, but cannot elicit a third peak. Shimoni *et al.*[3] can qualitatively explain the occurrence of discrete peaks. Further, our model incorporates the present damage level as a dynamic variable, whose reduction rate depends on the current activity of PolV and the damage level itself. In the Krishna *et al.*[2] model the rate of damage clearance is independent of the activity level of PolV. Connecting the activity level of the PolV repair response to the rate of damage repair should be an important feature of a model that describes the dynamic regulation of a repair response. Shimoni *et al.*[3] simply switch the damage level ON/OFF from outside the model.

Another difference between our model and that of Krishna *et al.*[2] is in the assumptions regarding the molecular mechanism leading to the occurrence of secondary expression peaks. In our model, we employed a regulatory delay, a feature readily encountered in molecular regulatory systems comprised of protein–protein interactions as well as transcriptional regulation. We assumed (based on a putative common dependence on protein synthesis, which is increasingly impaired

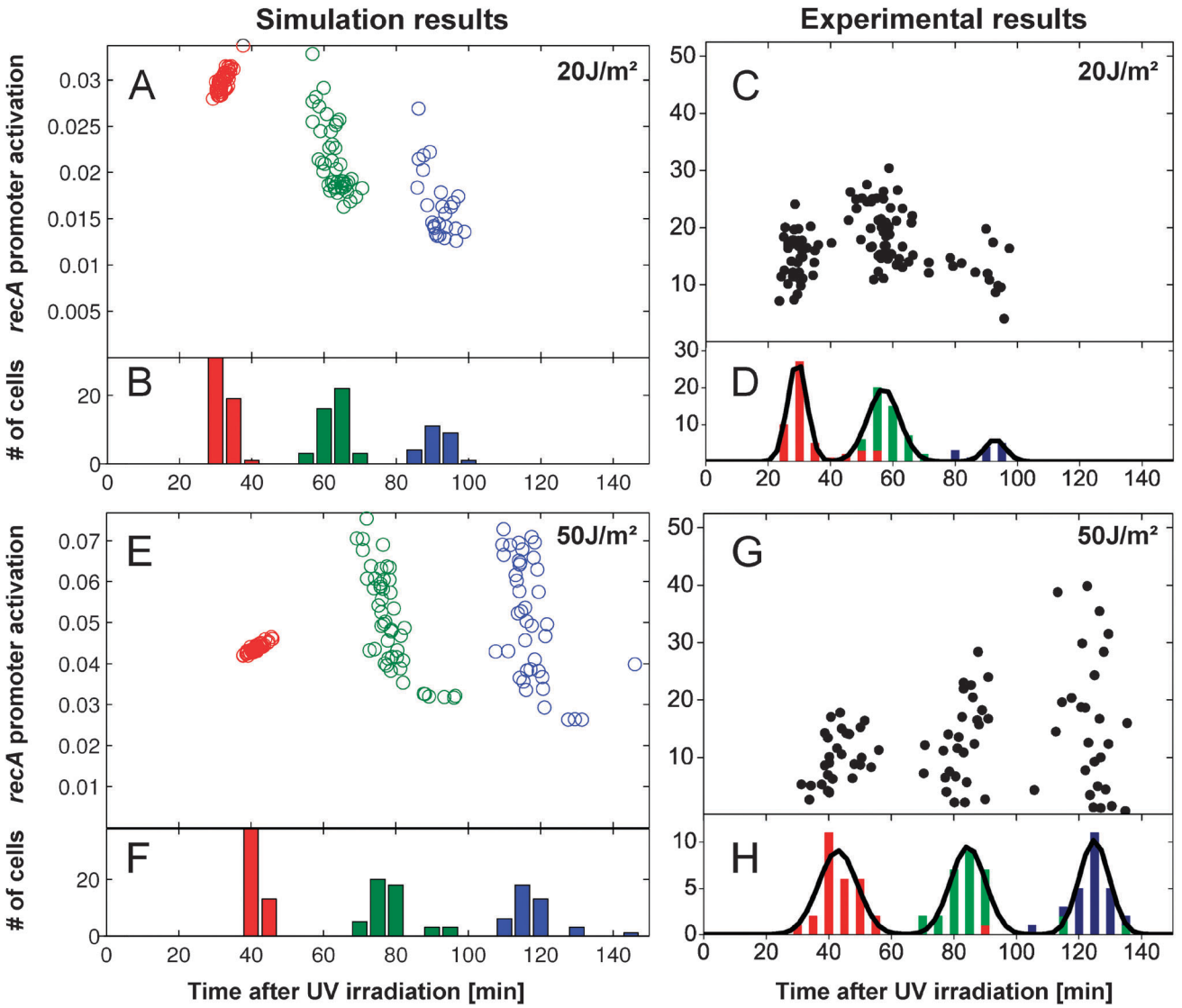

Fig. 2 *recA* expression peaks in simulation and experimental data from Friedman *et al.*[1] A: Each circle represents a *recA* expression peak amplitude in the model results (20 J m^{-2}) for 51 individual cells. Red circles are first peaks, green circles second peaks, and blue circles third peaks. B: Histograms of model result (20 J m^{-2}) peak times, colors same as in A. C: Experimental results (20 J m^{-2}) taken from Friedman *et al.*[1] Each circle represents a peak in *recA* promoter activity as measured by GFP expression. D: Histograms of experimental peak times (20 J m^{-2}), colors same as in A. E, F, G, H: Same as A, B, C, D (respective order) but UV dose 50 J m^{-2}.

by UV-induced damage) that the delay time τ depends on the cell doubling time T_D. Then, we adjusted the regulatory delay τ to fit the experimental data,[1] see Table 1; our delay times agree with the 7–10 minute delay between *recA* and *lexA* (most rapid expression response to stalled replication forks) and *umuDC* (encodes subunits of mutagenic SOS repair associated DNA polymerase V) promoter activity measured in experiment.[1] This experimentally found delay time was not used in formation of our model, rather the delay time τ was determined independently by matching our model to the available *recA* expression kinetics data. In contrast, Krishna *et al.* employ a hyper-sensitive threshold in relative concentrations of the UmuD and UmuC subunits to combine into active PolV. The threshold is associated with an abrupt assembly of PolV, which provides a molecular mechanism to "integrate" (in the mathematical sense of integration over time) *umuDC* expression as a signal to mutagenic SOS repair and trigger the second peak at a critical threshold. This is a strong assumption, and moreover necessary for the model of Krishna *et al.* to exhibit a second expression peak. A third peak does not arise from this assumption. The introduction of a delay makes this assumption unnecessary, a mechanistic interpretation of our model would actually indicate that PolV exerts repair action rapidly after *umuDC* expression.

Simplicity and number of parameters. The model presented in this paper employs two differential equations: a delay differential equation is the dynamical core of our model, and one ordinary differential equation is used to monitor the amount of DNA damage. These equations require exactly 6 parameters. while 3 more parameters are used to mimic biological variations, but these have no effect on the overall

This journal is © The Royal Society of Chemistry 2011

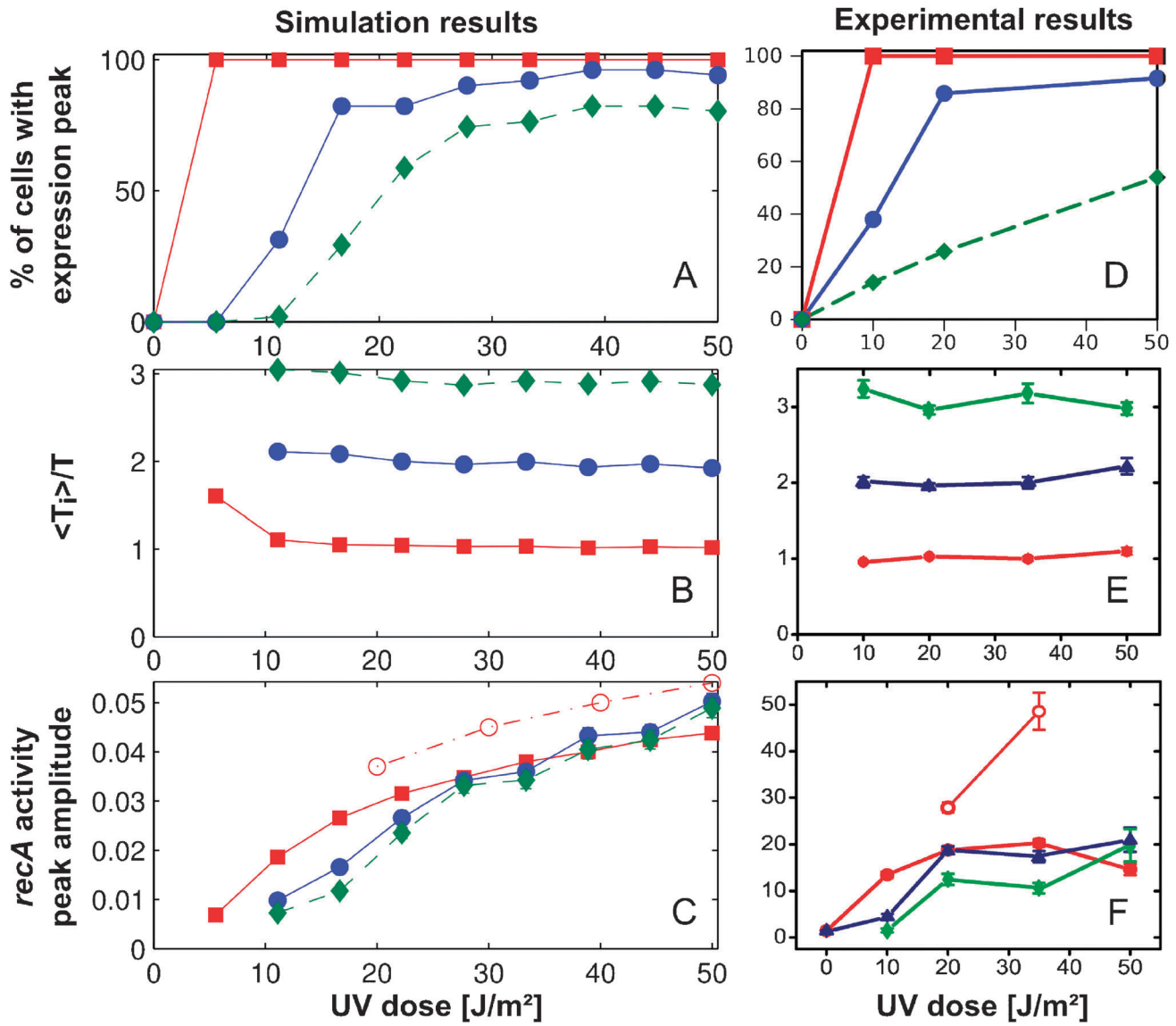

Fig. 3 Dependence of peak characteristics on UV irradiation dose. A, B, and C are from model simulations with 51 cells for each dose. The error bars, drawn from the standard error of the mean, partly vanish behind symbols. D, E and F display experimental results and are taken from Friedman *et al.*[1] Red always represents the first, blue the second, and green the third peak. A: Percentage of simulated cells exhibiting the according peak. B: Simulation peak times $\langle T_i \rangle$ scaled by $T(I)$. C: *recA* peak amplitudes in simulation. The dashed red line with hollow circles represents the first peak amplitude for the Δ*umu* knockout mutant. D: Same as A but from experimental data. E: Same as B but from experimental data. F: $\langle PA_i \rangle / PA_0$ peak amplitudes in experimental *recA* promoter activity. Hollow red circles represent experimental Δ*umu* promoter activity Peak 1 amplitudes.

dynamical behavior. Krishna *et al.*[2] build a complex regulatory network of 6 ODEs, one of which is reduced to its quasi-steady state. Shimoni *et al.*[3] claim to create a minimal model, using 18 model parameters in a stochastic simulation.

Model robustness. We introduce parameter fluctuations into our model simulation to account for biological variations. None of these variations qualitatively disrupts our model results. Also, discrete, correlated peaks are found in our model over a vast range of delay times; changing the other model parameters can affect the number and timing of peaks, but mostly does not affect the qualitative occurrence of discrete peaks either, as can be tried using our simulation code in the ESI.† This speaks of robust model behavior over a broad parameter space.

Insights, predictions and hypotheses. The aim of a minimal model is not primarily to give mechanistic insight into the underlying biochemistry. Rather, its strength should be in making a few conceptual points: The introduction of a strikingly simple delay model captures a great deal of the experimental behavior presented by Friedman *et al.*[1] While a minimal model like ours will not be sufficient to explain experimental findings in as much detail as a fully developed and biologically realistic one, the existent more complex models[2,3] without dynamical delay do not explain some important features present in the experimental data.[1] Delay models are a standard approach for

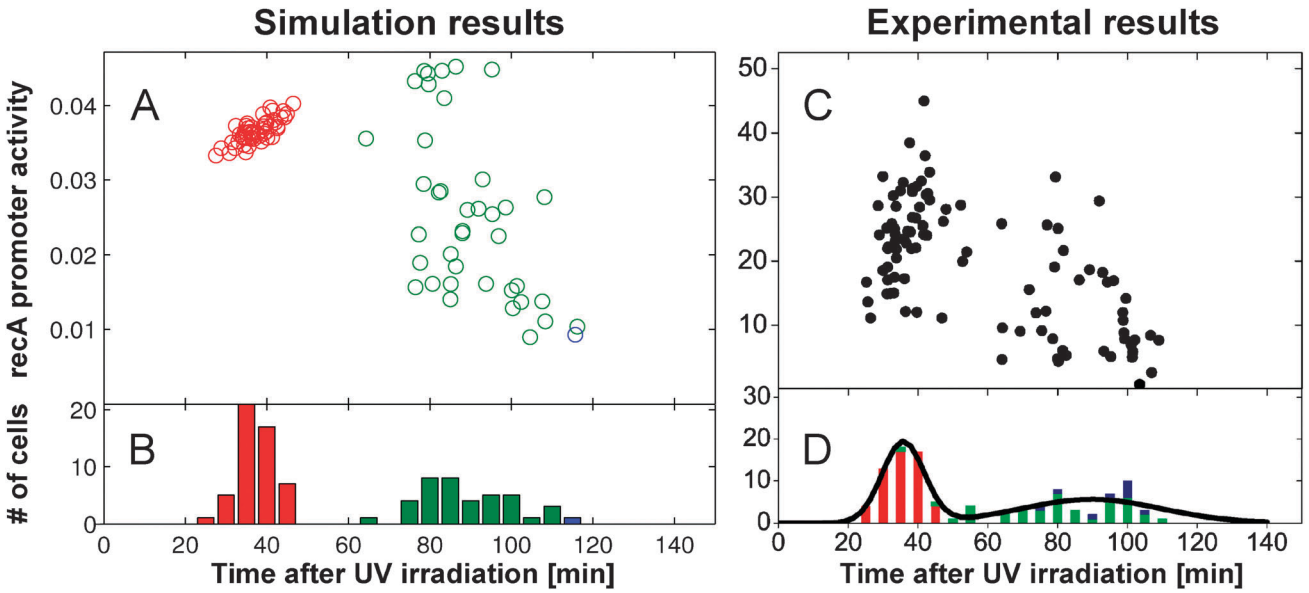

Fig. 4 Δ*umu* knockout mutant *recA* expression peaks in simulation and experimental data from Friedman *et al.*[1] A: Model results with delay time τ increased by 90% and increased variance of delay time variations $\sigma_\tau = 0.15$ at UV dose 20 J m^{-2}. Each circle represents a *recA* expression peak amplitude from one individual cell. Red circles are first peaks, green circles second peaks, and blue circles third peaks. 51 individual cells have been simulated. B: Histograms of model result peak times, colors same as in A. C: Experimental results taken from Friedman *et al.*[1] Each circle represents a peak in *recA* promoter activity as measured by GFP expression. D: Histograms of experimental peak times, colors same as in A.

multi-time scale dynamics. The SOS kinetics are governed by fast protein–protein interactions and slow gene regulatory effects, thus making SOS kinetics an ideal example of multi-time scale regulation. It is therefore not surprising that a delay model captures much of the experimentally observed regulation pattern. In contrast to claims made by Shimoni *et al.*[3] stochasticity seems unnecessary for a qualitative explanation of the observed SOS kinetics, though it might be of importance for a biologically realistic model. An in-depth description of the integration of delay and stochastic effects in a closely related regulatory system is presented by Liu *et al.*[16]

Our model development employs the hypothesis that the delay time τ, in close relation with the cell doubling time T_D, depends on the UV dose I. An increased cell doubling time can be understood as a proxy for slowed down protein synthesis, which in turn might also increase the delay time τ. We found the delay time τ to agree with the range of delay times between *recA* and *umuDC* promoter activity of 7–10 minutes. Investigating this experimentally detected delay time for dependence on the UV dose might yield a qualitative agreement with the dependence described by us, which would constitute a strong confirmation of our model and its basic assumptions. Given the feasibility of the original experiment,[1] this experimental knowledge should be easily accessible, or even be derived by the according analysis of the existent expression kinetics data.

Implications for *E. coli* SOS regulation

From our model, it seems likely that the whole *lexA*/*recA*/*umu* regulatory complex of the SOS response goes through delay-induced oscillations with an oscillation period equal to the peak separation time. In fact, this is the exact behavior present in the experimental data.[1] This interpretation is different from that of Krishna *et al.*,[2] who associate mutagenesis only with occurrence of the second *recA* expression peak. Our model associates all three *recA* expression peaks with signaling to mutagenic elements of the SOS response, while strong mutagenesis only occurs if heavy physical DNA damage persists up to the time of full assembly of PolV.

In accordance with the data of the Δ*umu* knockout mutant, prolonging the delay time by 90% and increasing the biological fluctuations captures the observed Δ*umu* kinetics,[1] see Fig. 4. This might point towards the activation of a redundant response to genome damage, which is masked in wild type cells by the action of PolV. Redundant pathways are readily encountered in molecular biology, and a regulatory function of UmuD and UmuC similar to a eukaryotic DNA damage checkpoint has been suggested.[17] This differs from the interpretation of Krishna *et al.*,[2] who explain the Δ*umu* data as a loss of the second *recA* expression peak that they associate with mutagenesis.

Broader implications

Our model gives a specific answer to the general question of how physiological priorities can manifest themselves in organismic regulation mechanisms. While the observed PolV expression oscillations might actually not hold physiological importance, they have indeed allowed us to uncover the potential role of a regulatory delay. In the specific example, the delayed activation of PolV allows the unicellular organism to react appropriately to two different scenarios of physical DNA damage, *cf.* also Friedman *et al.*:[1] (1) in case of little damage, non-mutagenic gene repair is able to clear damage before mutagenic repair action of PolV can take effect, or (2) in case of heavy physical damage, PolV overrides the priority of genetic information integrity for the sake of

This journal is © The Royal Society of Chemistry 2011

securing the usability of the physical information carrier itself. At the same time, persistent damage is repaired stepwise with control points to check if integrity has meanwhile been restored. This behavior can be readily explained by a delayed negative feedback loop and seems to be evolutionary favored over a reaction that simply correlates in intensity with the induced damage. The regulatory network controlling the SOS response could be established by several components of the SOS response itself as hypothesized already by Friedman *et al*.[1]

From a more conceptual perspective, a pattern of delay-regulated integration of several staggered responses emerges. The regulatory integration of such responses, spanning a trade-off spectrum between the capacity to fend off an environmental challenge and inflicted self-damage, might be of conceptual value in other defense systems. Examples coming to mind are innate *vs*. adaptive immune response and cellular apoptosis/autophagy decisions. Further, it has been suggested that eukaryotic cells possess functionally comparable inducible DNA repair mechanisms,[18] whose regulatory integration with other critical responses with negative secondary effects[16] should be highly interesting.

5 Author contributions

LH devised the detailed model, wrote and executed simulations and initiated and coordinated the project. DA assisted model interpretation and consolidation as a biochemical specialist. LH and DA wrote the manuscript, DA did the main part of the literature review. MCM supplied the formal foundations for the delay model and for analytical and numerical analysis, as well as academic supervision of the project.

Acknowledgements

Discussions with Jinzhi Lei and Tomas Gedeon contributed greatly to the authors' understanding of this work. Romain Yvinec's comments helped to improve the manuscript. We thank the anonymous reviewers for their comments.

Most of the figures displaying experimental results were copied from the article presenting the original data,[1] in compliance with that article's open access license.

This work was supported by the Natural Sciences and Engineering Research Council (NSERC, Canada), and the Mathematics of Information Technology and Complex Systems (MITACS, Canada). LH was supported with the J. P. Collip Fellowship of the McGill Faculty of Medicine and a studentship of the McGill University Health Centre Research Institute. LH and DA were each supported by a student fellowship and a traveling stipend of the Studienstiftung des deutschen Volkes.

References

1 N. Friedman, S. Vardi, M. Ronen, U. Alon and J. Stavans, *PLoS Biol*., 2007, **3**, e238.
2 S. Krishna, S. Maslov and K. Sneppen, *PLoS Comput. Biol*., 2007, **3**, e41.
3 Y. Shimoni, S. Altuvia1, H. Margalit and O. Biham, *PLoS One*, 2009, **4**, e5363.
4 M. Radman, *Basic Life Sci*., 1975, **5A**, 355–367.
5 B. Michel, *PLoS Biol*., 2005, **3**, e255.
6 L. K. Lewis, G. R. Harlow, L. A. Gregg-Jolly and D. W. Mount, *J. Mol. Biol*., 1994, **241**, 507–523.
7 A. Kuzminov, *Microbiol. Mol. Biol. Rev*., 1999, **63**, 751–813.
8 S. L. Lusetti and M. M. Cox, *Annu. Rev. Biochem*., 2002, **71**, 71–100.
9 M. Gonzalez and R. Woodgate, *Bioessays*, 2002, **24**, 141–148.
10 R. Galhardo, P. Hastings and S. Rosenberg, *Crit. Rev. Biochem. Mol. Biol*., 2007, **42**, 399–435.
11 I. Bjedov, O. Tenaillon, B. Gerard, V. Souza, E. Denamur, M. Radman, F. Taddei and I. Matic, *Science*, 2003, **300**, 1404–1409.
12 T. Erneux, *Applied Delay Differential Equations*, Springer, 2009.
13 L. F. Shampine, *Appl. Numer. Math*., 2005, **52**, 113–127.
14 R. Maithreye, R. R. Sarkar, V. K. Parnaik and S. Sinha, *PLoS One*, 2008, **13.3**, e2972.
15 R. R. Sarkar, R. Maithreye and S. Sinha, *J. Math. Biol*., 2010, 1–25.
16 B. Liu, S. Yan and Q. Wang, *Mol. BioSyst*., 2011, **7**, 457463.
17 T. Opperman, S. Murli, B. T. Smith and G. C. Walker, *Proc. Natl. Acad. Sci. U. S. A*., 1999, **96**, 9218–9223.
18 M. Eller, T. Maeda, C. Magnoni, D. Atwal and B. Gilchrest, *Proc. Natl. Acad. Sci. U. S. A*., 1997, **94**, 12627–12632.